

Design of Continuous Alternate Wheels for an Omnidirectional Mobile Robot

Jeong-keun Kim*, Kyung-Seok Byun**, Jae-Bok Song***

* Department of Mechatronics Engineering, Korea University, Seoul, Korea
(Tel : +82-2-929-8501; E-mail: rokmarines@korea.ac.kr)

** Mechatronics Center, Samsung Electronics Co., Suwon, Korea
(Tel : +82-31-200-2989; E-mail: ks1byun@kornet.net)

***Department of Mechanical Engineering, Korea University, Seoul, Korea
(Tel : +82-2-3290-3363 ; E-mail: jbsong@korea.ac.kr)

Abstract: Many types of omnidirectional wheels with passive rollers have gaps between rollers. Since these gaps cause a wheel to make discontinuous contact with the ground, they lead to vertical and/or horizontal vibrations during wheel operation. In addition, the radii of passive rollers are related to the height of a bump an omnidirectional wheel can surmount. In this research a new design of the alternate wheel is proposed. Because this wheel makes continuous contact with the ground and has alternating large and small rollers around the wheel, it is termed a continuous alternate wheel (CAW). In this paper a design procedure is also presented to determine the optimum number of rollers, the radii of rollers and the inside inclination angle of an outer roller for given design specifications. The CAW based on this design is compared to the existing alternate wheels in terms of design. Finally, an actual continuous alternate wheel is constructed to verify validity of the design guidelines.

Keywords: Continuous alternate wheels, Omnidirectional mobile robots, Passive rollers

1. INTRODUCTION

Applications of wheeled mobile robots have recently extended to service robots for the handicapped or the aged and industrial mobile robots working in various environments. The most popular wheeled mobile robots are equipped with two independent driving wheels. Since these robots possess 2 degrees-of-motion (DOFs), they can rotate about any point, but cannot perform sideways motion. To overcome this type of limitation on motion, mobile robots with steerable wheels were suggested. They allow both rotation and sideways motions but not simultaneously. If such robots are used as a service robot, for example, they may get in the way of persons they assist, and require unnecessarily large space or move along a complicated path when changing their direction. To cope with these problems, omnidirectional mobile robots were proposed. They are capable of arbitrary motion in an arbitrary direction without changing wheel directions, because they can achieve 3 DOF motion on a two-dimensional plane. Various types of omnidirectional mobile robots have been proposed so far; off-centered wheels [1], ball wheels [2], and universal wheels [3] are more popular among them.

The initial universal wheel design illustrated in Fig. 1a has multiple passive rollers whose axes are positioned tangent to the wheel circumference. Since this type of wheel makes discontinuous contact with the ground due to gaps between successive rollers, however, the robot platform suffers from vertical vibrations to some extent. To minimize a gap between rollers, various variations of universal wheels have been devised. In the Mecanum wheel [4] shown in Fig. 1b, rollers are arranged in such a way that contact between the wheel and the ground is continuous. In the double wheels [5] shown in Fig. 1c, wheels are arranged in an overlapping way. These types of wheels touch the ground continuously, but the points of contact with the ground are not continuous as seen in the figures. This discontinuous contact may cause horizontal vibrations [6]. The alternate wheel mechanism [7], [8] in Fig. 1d is another attempt to minimize a gap between rollers for reduction in horizontal and vertical vibrations. Contact points are in line, thus causing little horizontal vibration.

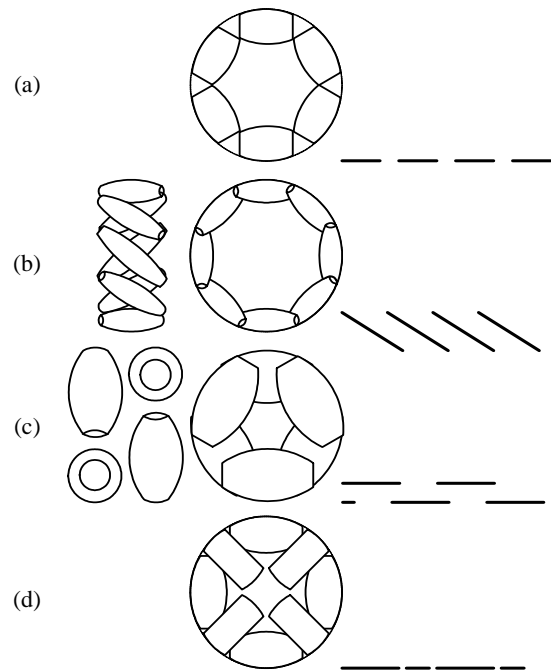


Fig. 1 Various wheel types using passive rollers and their traces; (a) classic, (b) Mecanum, (c) double, and (d) alternate.

Fig. 2 shows 2 types of alternate wheels in which large and small rollers (e.g., 8 rollers [7] and 12 rollers [8]) are alternated to reduce the gap size. Although many different alternate wheels have been designed so far, no systematic design guidelines for the number of rollers and the radii of rollers have been provided. These are important design factors in that the former is related to fabrication cost and the latter to the height of a surmountable bump.

3.1 Number and radii of rollers

Fig. 4 shows configuration of a proposed continuous alternate wheel (CAW) in which the inner and outer rollers alternate. As mentioned previously, the wheel contacts the ground continuously, since virtually no gap between rollers exists in this wheel. First, the conditions for no gap between rollers will be investigated below.

From the geometry in Fig. 4, the relationship between the wheel radius R and the half-angles θ_i and θ_o for the inner and outer rollers, respectively, becomes

$$2n(\theta_i + \theta_o) = 2\pi \quad (1)$$

where n represents the number of inner (or outer) rollers. If $n = 4$, for example, the wheel consists of 4 inner rollers and 4 outer rollers, and thus $\theta_i + \theta_o$ equals $\pi/4$. The center radius r_i and the end radius \hat{r}_i of an inner roller have the geometric relation

$$r_i = \hat{r}_i + R(1 - \cos \theta_i) \quad (2)$$

and the center radius r_o and the end radius \hat{r}_o of an outer roller have the similar relation

$$r_o = \hat{r}_o + R(1 - \cos \theta_o) \quad (3)$$

Spokes are used to support inner and outer rollers (See Fig. 8). The dimensions of a spoke such as width and thickness are determined depending on the maximum load the wheels are subject to. Some space margins between rollers are required for these spokes to be placed. As these margins get larger, fitting the spokes into the rollers gets easier at the cost of a smaller roller radius.

Let m_i be half the margin between inner rollers. Then the end radius of an inner roller for given m_i can be described by

$$(R \sin \theta_o - m_i) \geq 2\hat{r}_i \sin(\theta_i + \theta_o) \quad (4)$$

the end radius of an inner roller for given m_i is then obtained by

$$\hat{r}_i \leq \frac{R \sin \theta_o - m_i}{2 \sin(\theta_i + \theta_o)} \quad (5)$$

and thus the maximum \hat{r}_i becomes

$$\hat{r}_{i \max} = \frac{R \sin \theta_o - m_i}{2 \sin(\theta_i + \theta_o)}. \quad (6)$$

The maximum r_i is then easily computed by

$$r_{i \max} = \hat{r}_{i \max} + R(1 - \cos \theta_i). \quad (7)$$

Similarly, the end radius of an outer roller for given m_o is given by

$$\hat{r}_o \leq \frac{R \sin \theta_i - m_o}{2 \sin(\theta_i + \theta_o)} \quad (8)$$

where m_o is half the margin between outer rollers. The maximum end and center radii of an outer roller are then given by

$$\hat{r}_{o \max} = \frac{R \sin \theta_i - m_o}{2 \sin(\theta_i + \theta_o)}, \quad (9)$$

and

$$r_{o \max} = \hat{r}_{o \max} + R(1 - \cos \theta_o). \quad (10)$$

As shown in Fig. 4, some portion of an inner roller interpenetrates inside of an outer roller. The margin m_h is then needed for some portion of the spoke to reside between surfaces of the inner and outer rollers. The condition for the end radius of an outer roller for the given margin m_h is investigated below. First, let the xy coordinates be defined at the center of the wheel as shown in Fig. 4. The equation for the segment DE is given by

$$y = \frac{1}{\tan(\theta_i + \theta_o)}(x - R \sin \theta_i) + R \cos \theta_i \quad (11)$$

because the line DE passes the point D whose coordinate is $(R \sin \theta_i, R \cos \theta_i)$ and its slope is $1/\tan(\theta_i + \theta_o)$. The equation of the circle offset by the margin m_h from the surface of the inner roller (represented by the dashed arc MN) is described by

$$x^2 + \{y - (2R - 2r_i)\}^2 = (R + m_h)^2 \quad (12)$$

Solving Eqs. (11) and (12) yields the intersecting point P whose coordinates are

$$x_P = \frac{-ae \pm \{(a^2 + 1)f^2 - e^2\}^{1/2}}{a^2 + 1},$$

$$y_P = a(x_P - b) + c \quad (13)$$

where $a = 1/\tan(\theta_i + \theta_o)$, $b = R \sin \theta_i$, $c = R \cos \theta_i$, $d = 2R - 2r_i$, $e = -ab + c - d$, and $f = R + m_h$.

The segment DP must be less than or equal to the end diameter DE of an outer roller. Hence the minimum end radius of an outer roller is given by

$$\hat{r}_{o \min} = \frac{\{(R \sin \theta_i - x_P)^2 + (R \cos \theta_i - y_P)^2\}^{1/2}}{2} \quad (14)$$

The minimum center radius of an outer roller then becomes

$$r_{o \min} = \hat{r}_{o \min} + R(1 - \cos \theta_o) \quad (15)$$

In what follows, various design parameters are determined based on the above analysis. First, the margins were determined so that the roller radii become as large as possible by reducing the margins. They were selected as $m_i = 5.5\text{mm}$, $m_o = 4.5\text{mm}$, $m_h = 7.0\text{mm}$ for the wheel with a radius of $R = 10\text{cm}$ in the actual design.

Given a wheel radius R and the margins m_i , m_o , and m_h , the maximum and minimum radii of the inner and outer rollers can be determined as a function of θ_i (or, equivalently, θ_o) and n . Based on Eqs. (6), (7), (9), (10), and (15), the roller radii as a function of θ_i for $n = 3 \sim 8$ are illustrated in Fig. 5. In the figure, the maximum radius of an outer roller should be searched for in the region of $r_{o \max} \geq r_{o \min}$; otherwise, no solution exists. It is found that there is no solution for $n = 3$, since $r_{o \min}$ is greater than $r_{o \max}$ in the entire range of θ_i .

It is observed that as θ_i increases, the radii of the outer roller increase, but those of the inner roller decrease. Therefore, the maximum end radius of the inner roller $\hat{r}_{i \max}$ corresponds to the point where $r_{o \max} = r_{o \min}$ in the plots. Equating Eq. (10) to (15) yields

$$\frac{\{(R \sin \theta_i - x_P)^2 + (R \cos \theta_i - y_P)^2\}^{1/2}}{2} = \frac{R \sin \theta_i - m_o}{2 \sin(\theta_i + \theta_o)} \quad (16)$$

Since this equation cannot be solved explicitly, the numerical solution should be obtained.

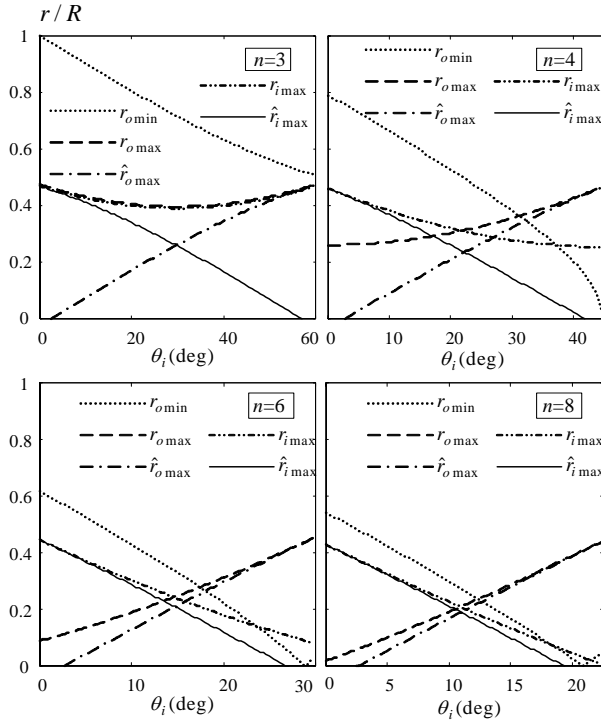


Fig. 5 Roller radii as a function of θ_i for various values of n

Table 1 Comparison of design parameters for various wheels

Parameters	[7]	CAW	[8]	CAW
n	4	4	6	6
R	10cm	10cm	10cm	10cm
θ_i	42.3°	31.2°	18.2°	17.4°
θ_o	12.7°	13.8°	11.8°	12.6°
ϕ	-	65.6°	-	65.7°
r_o	24.0mm	36.3mm	22.5mm	27.8mm
\hat{r}_o	16.5mm	33.4mm	19.5mm	25.4mm
r_i	12.0mm	27.4mm	15.0mm	20.9mm
\hat{r}_i	4.5mm	12.9mm	9.0mm	16.3mm

Table 1 compares the cases ($n = 4$ and 6) designed by the proposed method with those of References [7] and [8]. The roller radii increase by 150–280% for $n = 4$ and 120–180% for $n = 6$ for the same wheel radius. Fig. 5 shows the roller radii as a function of n . It is noted from the figure that for $n < 6$, the end radius of an inner roller gets smaller while the other radii get larger. For $n > 6$, all the radii tend to decrease, which is not desirable from the viewpoint of the height of a surmountable bump. Considering all these facts, the number of rollers was chosen as 6 in the design of a continuous alternate wheel. It is noted that the roller radii are maximized for given margins between rollers, and the inner and outer rollers are connected continuously along the wheel circumference.

4. CONSTRUCTION AND TESTS OF CONTINUOUS ALTERNATE WHEELS

4.1 Construction of CAW

An actual continuous alternate wheel was constructed based on the design parameters given in Table 1 ($n = 6$). The important dimensions of the wheel are shown in Fig. 6. In the

process of construction, more design factors other than the previously determined ones such as the number of rollers, roller radii, the interior inclination angle of an outer roller were considered. This section is concerned with the overall structure of a continuous alternate wheel.

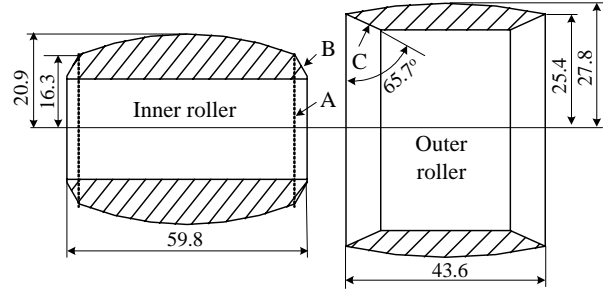
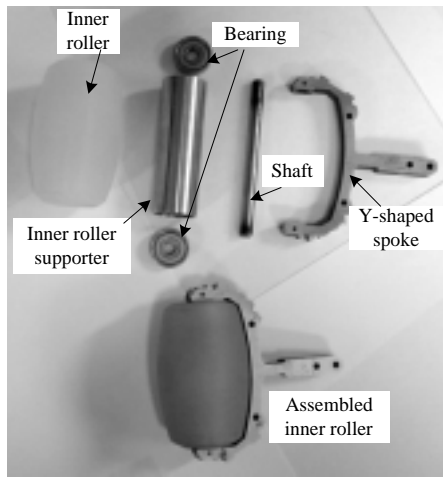


Fig. 6 Final shapes of inner and outer rollers

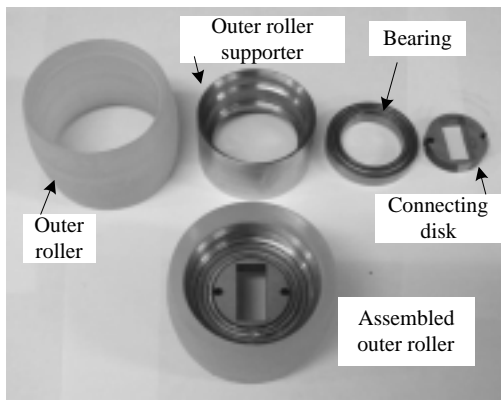
The shapes of inner and outer rollers designed in the previous section are capable of continuously contacting the ground without any interference between rollers. Polyurethane was selected as the roller material since it provides an appropriate friction coefficient and mechanical properties suited to an omnidirectional wheel. However, a urethane roller is not solid enough to prevent deformation when it is subject to loads due to contact with the ground. Therefore, steel supporters in the form of a hollow cylinder are inserted into the rollers to support urethane rollers.

Referring to Fig. 8, the fringe of the outer roller is relatively thin to avoid interference with the inner roller. This thin fringe, however, cannot be supported by any supporter, since the supporter may interfere with the inner roller. As a result, the thin fringe of the outer roller is not solid enough to bear the external load due to contact with the ground. To overcome this problem, the final shape of the rollers is designed as shown in Fig. 6. The inside surface of an outer roller forms a circular cone (denoted C in Fig. 6) with the inclination angle determined by the previous analysis. Note that another circular cone (denoted B) is added to the original sides of the inner roller (denoted A). These circular cones B and C do not contact each other when no external load is exerted on the wheel, since a small margin exists between the two surfaces. When the thin portion of the outer roller makes contact with the ground, however, surface C is pressed against surface B. Then, surface B supports surface C, and actually they rotate together about each roller axis. In this way, the problem of deformation of the fringe of an outer roller can be overcome without causing any interference with the inner roller.

A supporting structure is required to hold rollers around the wheel. The supporting parts for the inner roller are composed of a supporter, bearings, a shaft and a spoke, while those for the outer roller consist of a supporter, a bearing and a connecting disk as shown in Fig. 7. Fig. 8 shows a schematic diagram and a cutaway view of the final wheel and Fig. 9 is a photo of the finally assembled continuous alternate wheel. As shown in Fig. 8, the wheel has a hub with radially disposed six Y-shaped spokes made of stainless steel. Each spoke supports one inner roller through the roller axis with bearings at both ends.



(a) Parts of inner roller



(b) Parts of outer roller

Fig. 7 Photo of roller parts and assembled rollers

Two successive spokes, on the other hand, support the outer roller together through bearings. The total weight of a wheel is about 2.5kg. The payload of the omnidirectional robot with proposed wheels is about 100kg because it is designed to carry one person on it. Since the robot body weighs 49kg including 4 wheels, each wheel is designed to carry a vertical load of 50kg. FEM analysis was carried out to investigate deformation and strength of the wheel at the design stage of the wheel. Deformation and stress distributions for three parts - the inner roller, the overlap of the inner and outer rollers, and the outer roller – in contact with the ground were computed by the I-DEAS package while the wheel subject to a vertical load of 50kg rolls on the ground. Fig. 10 shows the stress distribution of the inner roller. From these distributions, the maximum deformations and stresses were found and listed in Table 2. A maximum deformation of 2.30mm occurs at the polyurethane of the outer roller. A maximum stress occurs at the supporter of the outer roller, but its value of 14.8MN/m² is far smaller than the yield strength of stainless steel (e.g., 200MN/m²). It follows from the FEM analysis that the designed wheels provide sufficient strength to carry the payload of 100kg. Actually, no problems have been found in the various tests in which an operator of the vehicle sits on the vehicle during its operation.

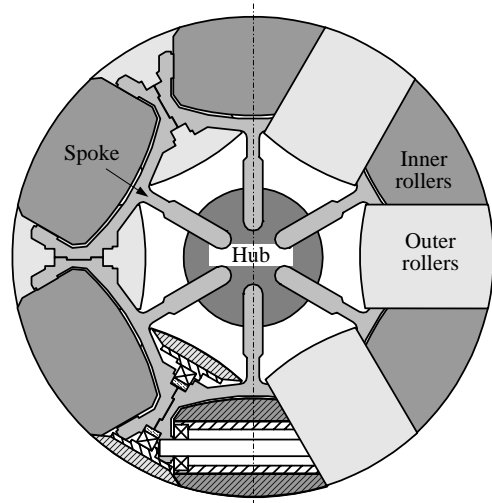


Fig. 8 Schematic diagram of proposed continuous alternate wheel



Fig. 9 Photo of constructed continuous alternate wheel

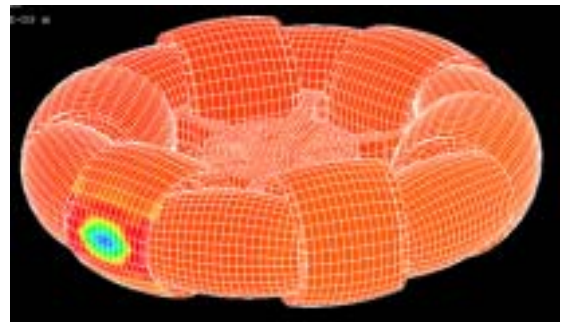


Fig. 10 Stress distribution of outer roller of wheel subject to a vertical load of 50kg

Table 2 Maximum deformations and stresses for various parts

Parts	Maximum deformation	Maximum stress
Inner roller	1.99mm	7.78MN/m ²
Overlap of two rollers	1.40mm	4.73MN/m ²
Outer roller	2.30mm	14.8MN/m ²

4.2 Tests

It is not easy to evaluate wheel performance during motion since it is impractical to place sensors on the passive rollers to measure their behavior. Because the CAWs are meaningful only when used in an omnidirectional vehicle, a prototype omnidirectional vehicle with 4 wheels shown in Fig. 11 has been built [9]. Each wheel module is composed of a CAW and a wheel motor. Since only 3 DOFs are required in an omnidirectional motion on the plane, 1 DOF is redundant and thus used for steering. Four wheel modules can steer about each pivot point located at the corners of the vehicle body, but they are constrained to have a synchronized steering motion of 1 DOF (i.e., identical magnitudes of all 4 steering angles) by the synchronous mechanism comprising a linear guide and connecting links. In summary, a combination of 4 independent control of wheels generates an omnidirectional motion.

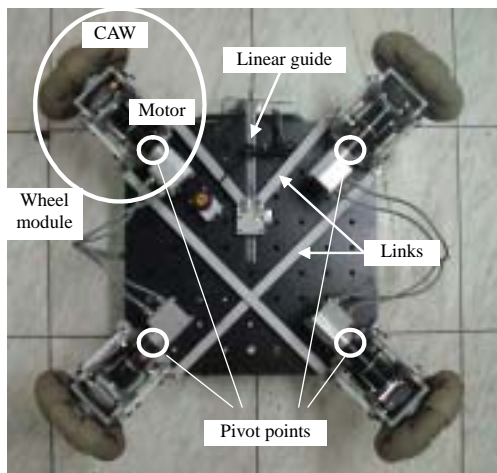


Fig. 11 Bottom view of prototype vehicle with CAWs

Some performance tests for the prototype vehicle have been conducted. Tracking performance of the vehicle with one person on it has been tested for various trajectories. Given a circular reference trajectory represented in the dashed line in Fig. 12, the vehicle control algorithm generates the required vehicle velocity and then computes the velocity of each wheel to achieve the desired motion through the Jacobian analysis. In the figure, the triangle indicates the position and orientation of a vehicle. The vehicle front is always directed toward the center of a circular path during motion, which is not feasible in the conventional vehicles. It is seen that the actual trajectory represented in the solid line tracks the reference reasonably well. Some error is observed around the finish since the prototype vehicle does not implement any position control algorithm for this test and thus position error has been accumulated during motion.

5. CONCLUSION

In this research a new design of a continuous alternate wheel (CAW) was proposed to minimize a gap between rollers and to maximize radii of rollers. The gap causes vertical and/or horizontal vibrations in many types of omnidirectional wheels with passive rollers, and roller radii are related to the height of a surmountable bump. This wheel is an improved version of a conventional alternate wheel where inner and outer rollers are disposed alternately.

This paper details the systematic design procedure of the continuous alternate wheel. That is, the design guidelines were presented to determine the optimum number of rollers, the radii of rollers, and the inside inclination angle of an outer

roller for given design specifications. It is shown that the proposed continuous alternate wheel can provide larger radii of the roller for the same size of the wheel than already existing alternate wheels.

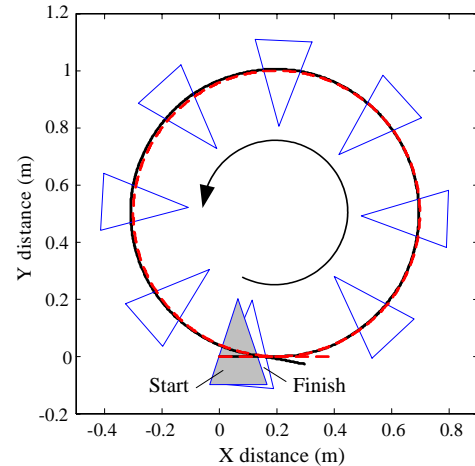


Fig. 12 Experimental results of tracking performance for a circular trajectory (solid line: actual trajectory, dashed line: reference trajectory)

Using the polyurethane rollers, the actual continuous alternate wheel was constructed to verify validity of the design guidelines. The omnidirectional mobile robots equipped with these proposed wheels were built and their tracking performance for various trajectories was evaluated.

ACKNOWLEDGEMENTS

This work was supported by Korea Research Foundation Grant (KRF-2002-041-D00038).

REFERENCES

- [1] M. Wada and S. Mory, "Holonomic and omnidirectional vehicle with conventional tires," *Int. Conf. on Robotics and Automation*, 1996, pp.3671-3676.
- [2] M. West, and H. Asada, "Design of ball wheel mechanisms for omnidirectional vehicles with full mobility and invariant kinematics," *Journal of Mechanical Design*, 1997, Vol. 119, pp.153-161.
- [3] J.F. Blumrich, "Omnidirectional vehicle," *United States Patent 3,789,947*, 1974.
- [4] B.E. Ilou "Wheels for a course stable self-propelling vehicle movable in any desired direction on the ground or some other base," *United States Patent 3,876,255*, 1975.
- [5] H. Asada, M. Sato and L. Bogoni, "Holonomic and omnidirectional vehicle with conventional tires," *Int. Conf. on Robotics and Automation*, 1995, pp.1925-1930.
- [6] L. Ferriere, B. Raucant, and G. Campion, "Design of omni-mobile robot wheels," *Int. Conf. on Robotics and Automation*, 1996, pp.3664-3670.
- [7] C. Fuchs, "The wheel that enables to move immediately in every direction," *Germany Patent 822,660*, 1951.
- [8] H. Asama, M. Sato, N. Goto, A. Matsumoto, and I. Endo, "Mutual transportation of cooperative mobile robots using forklift mechanisms," *Int. Conf. on Robotics and Automation*, 1996, pp.1754-1759.
- [9] K.-S. Byun, S.-J. Kim, and J.-B. Song, "Design of a Four-Wheeled Omnidirectional Mobile Robot with Variable Wheel Arrangement Mechanism," *Int. Conf. on Robotics and Automation*, 2002, pp., 720-725.